

See discussions, stats, and author profiles for this publication at: <https://www.researchgate.net/publication/236638550>

# Astrocyte-derived ATP modulates depressive-like behaviors

Article in *Nature medicine* · May 2013

DOI: 10.1038/nm.3162 · Source: PubMed

CITATIONS

178

READS

628

18 authors, including:



**Xiong Cao**

Southern Medical University

16 PUBLICATIONS 671 CITATIONS

SEE PROFILE



**Shu-Ji Li**

23 PUBLICATIONS 778 CITATIONS

SEE PROFILE



**Xin-Hong Zhu**

Southern Medical University

27 PUBLICATIONS 1,181 CITATIONS

SEE PROFILE



**Tian-Ming Gao**

Southern Medical University

118 PUBLICATIONS 2,496 CITATIONS

SEE PROFILE

# Astrocyte-derived ATP modulates depressive-like behaviors

Xiong Cao<sup>1-3</sup>, Liang-Ping Li<sup>1,2</sup>, Qian Wang<sup>1,2</sup>, Qiong Wu<sup>1,2</sup>, Hong-Hai Hu<sup>1,2</sup>, Meng Zhang<sup>1,2</sup>, Ying-Ying Fang<sup>1,2</sup>, Jie Zhang<sup>1,2</sup>, Shu-Ji Li<sup>1,2</sup>, Wen-Chao Xiong<sup>1,2</sup>, Hua-Cheng Yan<sup>1,2</sup>, Yu-Bo Gao<sup>1,2</sup>, Ji-Hong Liu<sup>1,2</sup>, Xiao-Wen Li<sup>1,2</sup>, Li-Rong Sun<sup>1,2</sup>, Yuan-Ning Zeng<sup>1,2</sup>, Xin-Hong Zhu<sup>1-3</sup> & Tian-Ming Gao<sup>1,2</sup>

Major depressive disorder (MDD) is a cause of disability that affects approximately 16% of the world's population<sup>1</sup>; however, little is known regarding the underlying biology of this disorder. Animal studies, postmortem brain analyses and imaging studies of patients with depression have implicated glial dysfunction in MDD pathophysiology<sup>2-7</sup>. However, the molecular mechanisms through which astrocytes modulate depressive behaviors are largely uncharacterized. Here, we identified ATP as a key factor involved in astrocytic modulation of depressive-like behavior in adult mice. We observed low ATP abundance in the brains of mice that were susceptible to chronic social defeat. Furthermore, we found that the administration of ATP induced a rapid antidepressant-like effect in these mice. Both a lack of inositol 1,4,5-trisphosphate receptor type 2 and transgenic blockage of vesicular gliotransmission induced deficiencies in astrocytic ATP release, causing depressive-like behaviors that could be rescued via the administration of ATP. Using transgenic mice that express a  $G_q$  G protein-coupled receptor only in astrocytes to enable selective activation of astrocytic  $Ca^{2+}$  signaling, we found that stimulating endogenous ATP release from astrocytes induced antidepressant-like effects in mouse models of depression. Moreover, we found that P2X2 receptors in the medial prefrontal cortex mediated the antidepressant-like effects of ATP. These results highlight astrocytic ATP release as a biological mechanism of MDD.

The chronic social defeat stress (CSDS) model mimics several psychopathological dimensions of depression, and adult C57BL/6J mice that are subjected to CSDS can be separated into susceptible and unsusceptible subpopulations<sup>8,9</sup> (Supplementary Fig. 1a and Supplementary Methods). To characterize the neurobiological mechanisms that underlie astrocyte dysfunction in depression, we analyzed the amounts of peptide trophic factors and neurotransmitters that are known to be secreted by astrocytes in the prefrontal cortex (PFC) and hippocampus, two candidate sites for impaired functions in MDD<sup>6,10</sup>, in mice subjected to CSDS (Supplementary Fig. 1b). Notably, the

concentration of ATP was lower in the artificial cerebral spinal fluid (ACSF) from PFC or hippocampal slices that were isolated from susceptible but not unsusceptible mice when compared with nondefeated control mice (Fig. 1a), suggesting an ATP deficiency in the brains of mice that are sensitive to CSDS. To determine whether ATP deficiency underlies acute behavioral despair, we used the forced swimming test (FST). We found that ATP amounts were lower in the brains of mice subjected to a 6-min FST when compared with undisturbed control mice (Fig. 1b). Further *in vivo* microdialysis experiments demonstrated that ATP concentrations in the interstitial fluid were lower in the PFC and hippocampus of the mice that were susceptible to CSDS (Fig. 1c). Together, these results suggest that reduced levels of ATP in the brain underlie depressive-like behaviors.

To test whether ATP could induce an antidepressant-like effect, we employed the FST (Supplementary Fig. 2a). A physiological concentration of ATP (25  $\mu$ M, lateral intracerebroventricular (i.c.v.) infusion)<sup>11</sup> decreased the total duration of immobility in adult C57BL/6J mice. Moreover, ATP- $\gamma$ -S, a nonhydrolyzable ATP analog, dramatically decreased the total duration of immobility, excluding the possible contribution of ATP hydrolysis products. Notably, the effects of ATP and ATP- $\gamma$ -S were blocked by a preinfusion of suramin, a broad purinergic P2 receptor antagonist<sup>12</sup> (Fig. 1d). These treatments had no effect on locomotor activity (Supplementary Fig. 3a), indicating that ATP could have antidepressant-like effects. We then considered whether ATP could reverse CSDS-induced social avoidance, which is a model of stress-induced psychopathology in humans<sup>8,9</sup>. In the CSDS experiments, neither the ATP nor the ATP- $\gamma$ -S infusion had any effect on the duration of time that nondefeated mice spent in the interaction zone when a caged aggressor was introduced into the test area (Supplementary Fig. 2b). After a 10-d CSDS protocol, the mice that were treated with vehicle exhibited an approximately 70% reduction in time spent in the interaction zone. In contrast, a 7-d treatment with ATP or ATP- $\gamma$ -S reversed the defeat-related behaviors in mice after CSDS (Fig. 1e), suggesting that ATP induces antidepressant-like effects in adult mice.

Classical antidepressants are generally administered via intraperitoneal (i.p.) injection to experimental animals. Therefore, to compare the efficiency and onset time of ATP with those of classical

<sup>1</sup>Department of Neurobiology, School of Basic Medical Sciences, Southern Medical University, Guangzhou, China. <sup>2</sup>Key Laboratory of Neuroplasticity of Guangdong Higher Education Institutes, Southern Medical University, Guangzhou, China. <sup>3</sup>School of Traditional Chinese Medicine, Southern Medical University, Guangzhou, China. Correspondence and requests for materials should be addressed to X.-H.Z. (zhuxh@smu.edu.cn) or T.-M.G. (tgao@smu.edu.cn).

Received 12 July 2012; accepted 15 March 2013; published online 5 May 2013; doi:10.1038/nm.3162

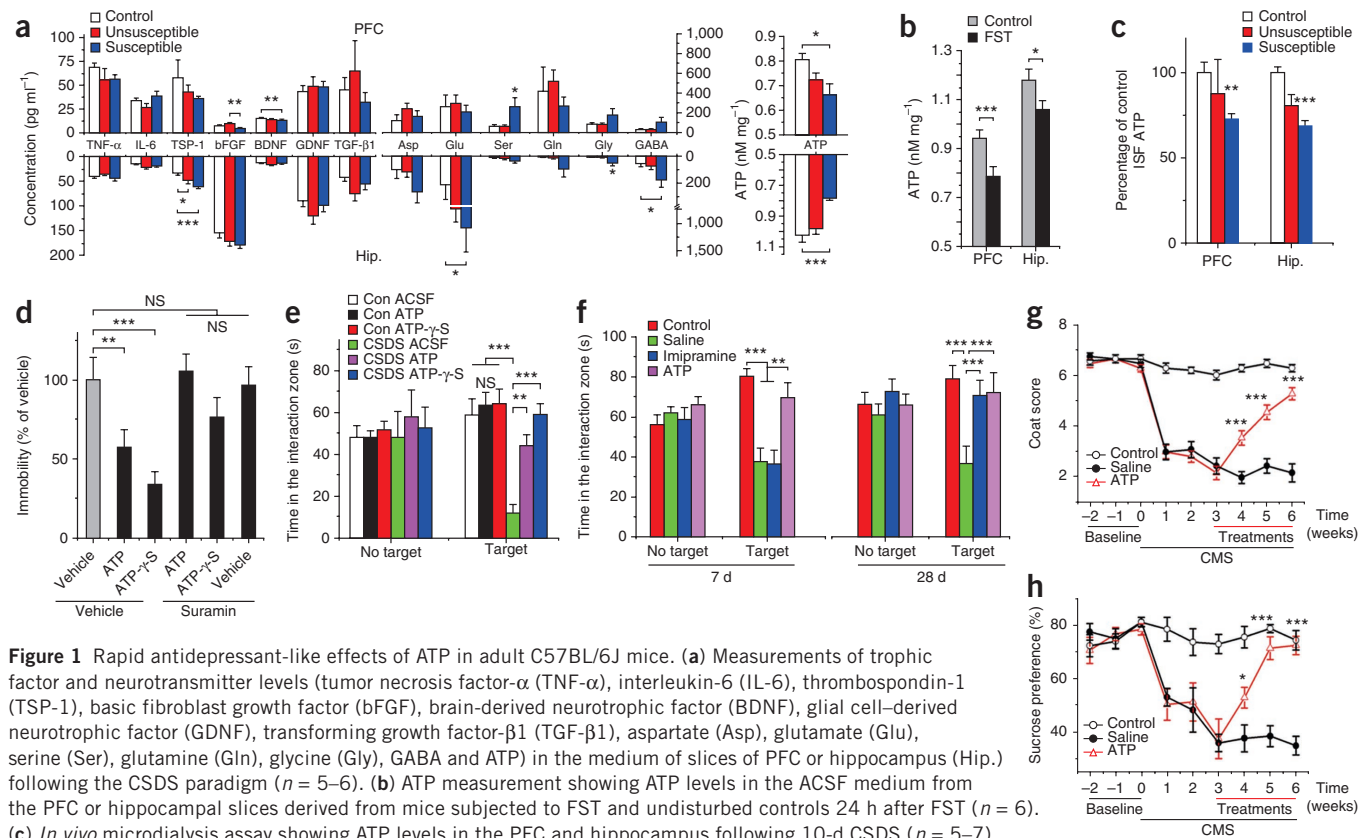


**Figure 1** Rapid antidepressant-like effects of ATP in adult C57BL/6J mice. **(a)** Measurements of trophic factor and neurotransmitter levels (tumor necrosis factor-α (TNF-α), interleukin-6 (IL-6), thrombospondin-1 (TSP-1), basic fibroblast growth factor (bFGF), brain-derived neurotrophic factor (BDNF), glial cell-derived neurotrophic factor (GDNF), transforming growth factor-β1 (TGF-β1), aspartate (Asp), glutamate (Glu), serine (Ser), glutamine (Gln), glycine (Gly), GABA and ATP) in the medium of slices of PFC or hippocampus (Hip.) following the CSDS paradigm ( $n = 5-6$ ). **(b)** ATP measurement showing ATP levels in the ACSF medium from the PFC or hippocampal slices derived from mice subjected to FST and undisturbed controls 24 h after FST ( $n = 6$ ). **(c)** *In vivo* microdialysis assay showing ATP levels in the PFC and hippocampus following 10-d CSDS ( $n = 5-7$ ). **(d)** Quantification of the total duration of immobility as a percentage of the vehicle after i.c.v. infusion of ATP or ATP-γ-S ( $n = 10$ ). **(e)** Interaction zone times for the controls and mice treated with ATP or ATP-γ-S (i.c.v.) in conditions of no target and CD1 target ( $n = 10-12$ ). **(f)** The avoidance behaviors for the mice after 7-d or 28-d treatment with saline, imipramine or ATP (i.p.) ( $n = 10-12$ ). **(g, h)** CMS paradigm. Measurements of the physical state of the coat **(g)** and the sucrose preference **(h)** showing baseline followed by post-stress measurements conducted each week for the controls and mice treated with saline or ATP (repeated measures,  $n = 11$ ). ANOVA followed by least significant difference (LSD) *post hoc* test: \* $P < 0.05$ , \*\* $P < 0.01$ , \*\*\* $P < 0.001$ . NS, not significant. Data are expressed as the means  $\pm$  s.e.m.

antidepressants, we sought to determine whether an i.p. injection of ATP could induce antidepressant-like effects. Similar to the results that were observed for the i.c.v. ATP infusion, an i.p. ATP injection of 125 mg per kg body weight, which could increase ATP abundance in the brain, decreased the duration of immobility without affecting locomotor activity in adult C57BL/6J mice (**Supplementary Figs. 3b** and **4**). Of note, in the CSDS paradigm (**Supplementary Fig. 2c**), a 7-d treatment with ATP was sufficient to stably reverse avoidance behaviors in defeated mice (**Fig. 1f**). Consistent with previous reports<sup>8,9</sup>, we observed that a 4-week treatment with the well-characterized antidepressant imipramine was necessary to increase the interaction time of defeated mice to the levels that we observed in control mice, whereas a 1-week treatment with imipramine was ineffective, which suggests that ATP may be a faster-acting antidepressant (**Fig. 1f**).

To further characterize the rapid antidepressant-like effects of ATP in mice with depressive-like behavior, we employed another widely used mouse model of depression: the chronic mild stress (CMS) paradigm<sup>13</sup> (**Supplementary Fig. 2d**). In agreement with previous reports, the CMS paradigm resulted in coat deterioration (**Fig. 1g**) and decreased sucrose preference in saline-treated mice (**Fig. 1h**)<sup>13,14</sup>. In contrast, ATP administration markedly improved the physical state of the coat and increased sucrose preference in mice with depressive-like behavior within 7 d after the treatment (**Fig. 1g,h**). These results further support the hypothesis that ATP can induce rapid-onset, antidepressant-like effects.

It has been demonstrated that astrocytic release of ATP is triggered by increases in intracellular calcium concentrations ( $[Ca^{2+}]_i$ )<sup>15-19</sup>. These increases are predominantly elicited via the inositol 1,4,5-trisphosphate (IP3) pathway. Because IP3 receptor type 2 (IP3R2) is the only astrocyte-specific functional IP3R isoform<sup>15-20</sup>, we used *Itpr2* knockout (*Itpr2*<sup>-/-</sup>) mice to modulate astrocytic ATP release *in vivo*. We consistently observed that the deletion of *Itpr2* selectively disrupted astrocyte function, as bath application of a G<sub>q</sub> G protein-coupled receptor (GPCR) agonist cocktail could elicit  $[Ca^{2+}]_i$  responses in cultured neurons, but not in astrocytes derived from the brains of *Itpr2*<sup>-/-</sup> mice (**Supplementary Figs. 5 and 6**)<sup>20,21</sup>. Notably, ATP concentrations were lower in the ACSF from the PFC and hippocampal slices derived from *Itpr2*<sup>-/-</sup> mice as compared with wild-type mice (**Fig. 2a**). Moreover, ATP concentrations were markedly decreased in the culture medium of astrocytes isolated from *Itpr2*<sup>-/-</sup> mice. However, neuronal ATP release was undisturbed by the lack of *Itpr2* (**Fig. 2b**), indicating that ATP release specifically from astrocytes was deficient in *Itpr2*<sup>-/-</sup> mice.

We next tested whether *Itpr2*<sup>-/-</sup> mice exhibited depressive-like behaviors. In the FST, the duration of immobility increased in *Itpr2*<sup>-/-</sup> mice compared with controls (**Fig. 2c**). Furthermore, *Itpr2*<sup>-/-</sup> mice had deteriorated coats (**Fig. 2d**) and consumed less sucrose solution than controls (**Fig. 2e**). No differences were observed between the two groups in the open-field test, the elevated-plus-maze test, the total solution intake and the sleep-wake profiles (**Supplementary Figs. 7-12**). These observations imply that a lack of *Itpr2* could induce depressive-like behaviors in adult mice.

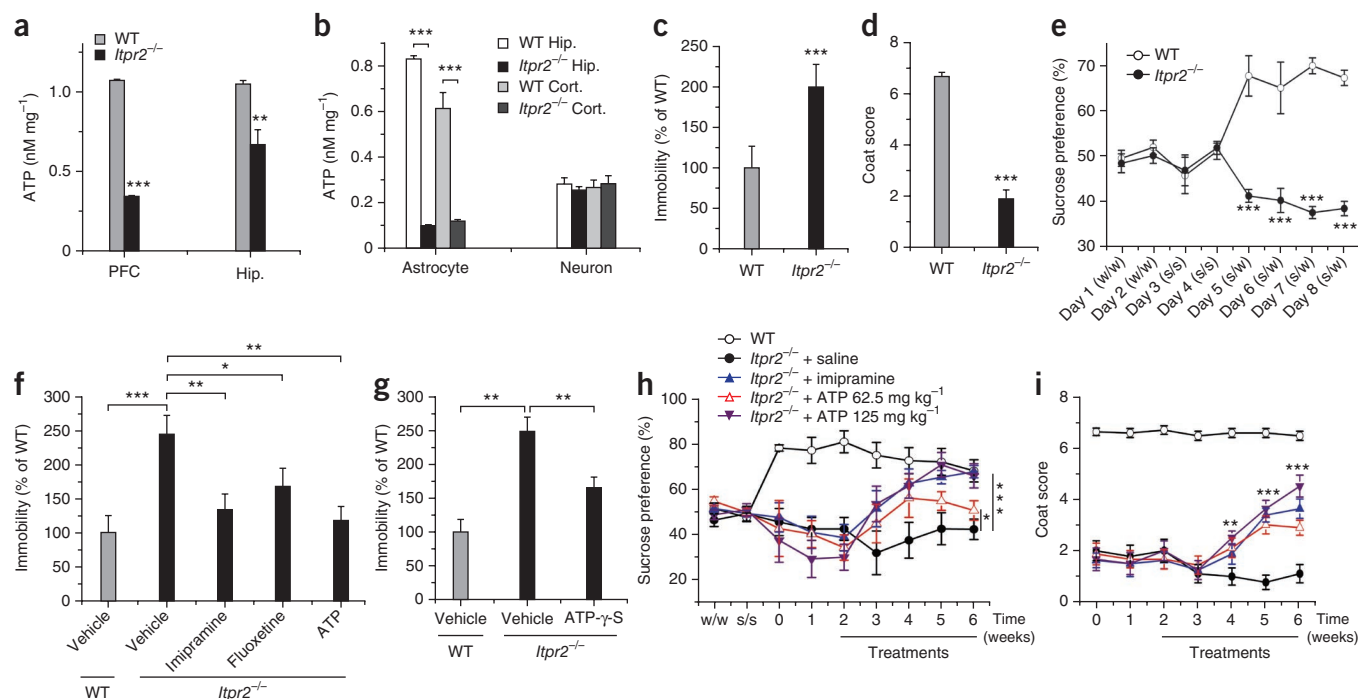


**Figure 2** The lack of *Itpr2* affects astrocytic ATP release, induces depressive-like behaviors and can be rescued via ATP administration. **(a)** ATP measurements showing ATP levels in the media of slices of PFC or hippocampus that were isolated from *Itpr2*<sup>-/-</sup> mice ( $n = 6$ ). **(b)** ATP levels in cultured astrocytes ( $n = 7$  or  $8$ ) or neurons ( $n = 6$ ) isolated from *Itpr2*<sup>-/-</sup> mice and controls (WT). Cort., cortex. **(c–e)** Behavioral changes of *Itpr2*<sup>-/-</sup> mice in the FST ( $n = 11$ ) **(c)**, the coat score assay ( $n = 9$ ) **(d)** and the sucrose preference test (repeated measures,  $n = 12$ ) **(e)**. w/w, water/water; s/s, sucrose/sucrose; s/w, sucrose/water. **(f)** Quantification of the immobility for the *Itpr2*<sup>-/-</sup> mice and controls treated with vehicle, ATP, imipramine or fluoxetine (i.p.) ( $n = 9$  or  $10$ ). **(g)** The effect of i.c.v. infusions of ATP-γ-S on the increased immobility that was observed in *Itpr2*<sup>-/-</sup> mice in the FST ( $n = 8–10$ ). **(h,i)** Sucrose preference test and coat score assay for the *Itpr2*<sup>-/-</sup> mice treated with saline, imipramine or ATP (repeated measures,  $n = 8–10$ ). ANOVA followed by LSD *post hoc* test: \* $P < 0.05$ , \*\* $P < 0.01$ , \*\*\* $P < 0.001$ . Data are expressed as the means  $\pm$  s.e.m.

We then examined whether the administration of ATP could ameliorate depressive-like behaviors in *Itpr2*<sup>-/-</sup> mice. Acute treatment with either imipramine or fluoxetine prevented the increased immobility that was observed in untreated *Itpr2*<sup>-/-</sup> mice, indicating that *Itpr2*<sup>-/-</sup> mice respond to antidepressants frequently prescribed to humans. We observed an equivalent behavioral response following an ATP injection (125 mg per kg body weight, i.p., Fig. 2f). In a parallel series of experiments, an i.c.v. infusion of ATP-γ-S blocked the increased duration of immobility (Fig. 2g). In contrast, infusion of adenosine, an ATP hydrolysis product, worsened the depressive-like behavior of *Itpr2*<sup>-/-</sup> mice. The infusion of ATP-γ-S or adenosine had no effect on locomotor activity (Supplementary Fig. 13), indicating that it was ATP, not adenosine, that rescued depressive-like behaviors in *Itpr2*<sup>-/-</sup> mice. Furthermore, we tested whether ATP could rescue depressive-like behaviors in *Itpr2*<sup>-/-</sup> mice as measured by the coat score assay and sucrose intake tests (Supplementary Fig. 2e). A 3-week imipramine treatment significantly increased sucrose preference (Fig. 2h) and improved the physical state of the coat (Fig. 2i). ATP administration induced antidepressant-like effects in a dose-dependent manner. Moreover, a 3-week treatment with ATP (125 mg per kg body weight, i.p.) completely reversed the deficiencies of *Itpr2*<sup>-/-</sup> mice in the sucrose preference test ( $P = 0.983$  versus controls) (Fig. 2h). These results suggest that a deficiency in astrocytic ATP release is the cause of depressive-like behaviors in *Itpr2*<sup>-/-</sup> mice.

Astrocyte-specific transgenic expression of a dominant-negative form of the soluble *N*-ethylmaleimide-sensitive factor attachment protein receptor (dn-SNARE) domain of synaptobrevin 2 is presumed to inhibit astrocytic exocytosis of ATP<sup>22</sup>. To further determine whether

deficient astrocytic release of ATP causes depressive-like behaviors, we examined the behaviors of dn-SNARE mice, in which expression of the dn-SNARE domain of synaptobrevin 2 can be suppressed by doxycycline<sup>22</sup>. After finding that astrocytic ATP release was deficient in dn-SNARE mice (Fig. 3a), we subjected these mice and the controls to the FST. The dn-SNARE mice exhibited more immobility compared with both wild-type mice and tetracycline transactivator (tTA) single-transgenic mice; this increase was completely blocked by the addition of doxycycline to the drinking water. This result suggests that astrocytic dysfunction causes depressive-like behaviors in dn-SNARE mice. Most importantly, ATP administration (125 mg per kg body weight, i.p.) completely reversed the increased immobility in dn-SNARE mice (Fig. 3b). No differences were observed in the open-field test between dn-SNARE mice and controls (Supplementary Fig. 14a). These data further support the hypothesis that deficient astrocytic ATP release causes depressive-like behaviors in adult mice.

To determine whether the enhancement of endogenous astrocytic ATP release was sufficient to induce antidepressant-like effects in mice with depressive-like behaviors, we generated mice transgenic for Mas-related gene A1 (official symbol *Mrgpra1*; here called MrgA1<sup>+</sup> mice) by crossing GFAP:tTA mice with tetO.MrgA1 mice. In MrgA1<sup>+</sup> mice, the functional MrgA1 receptor, a G<sub>q</sub> GPCR normally expressed in specific subsets of nociceptive sensory neurons in the spinal cord, is specifically expressed in astrocytes to enable selective activation of G<sub>q</sub> GPCR Ca<sup>2+</sup> signaling following infusion of the MrgA1 receptor agonist peptide Phe-Leu-Arg-Phe amide (FLRFα)<sup>21,23,24</sup>. We confirmed that the GFP-tagged MrgA1 receptors were selectively expressed in astrocytes. Furthermore, FLRFα application resulted in a

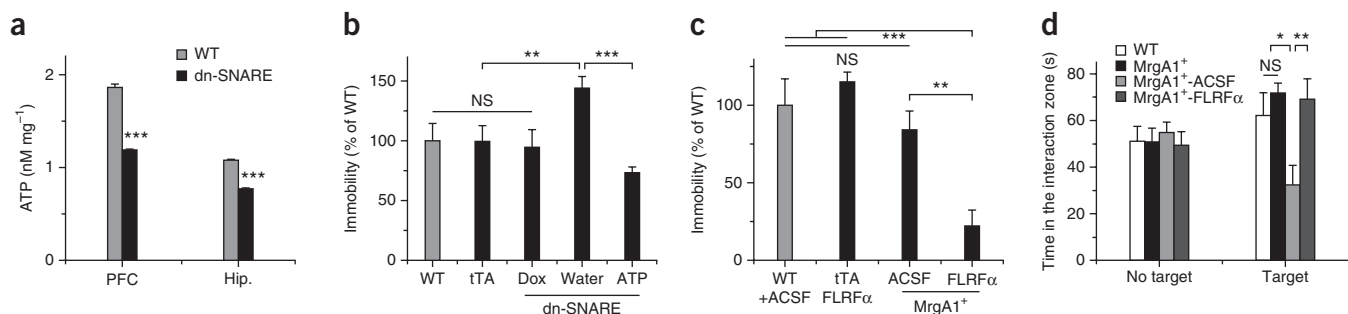


**Figure 3** Behavioral changes following endogenous modulation of astrocytic ATP release. (a) ATP measurements showing ATP levels in the media of slices of the PFC or hippocampus isolated from dn-SNARE mice ( $n = 6$ ). (b) Quantification of the immobility for WT, tTA control (tTA) and dn-SNARE mice treated with doxycycline (Dox) or ATP ( $n = 10$ ). (c) The effect of an infusion of FLRF $\alpha$  (i.c.v.) on the immobility in Mrg1 $^{+}$  mice in the FST ( $n = 8$ ). (d) Interaction zone times for controls (WT) and Mrg1 $^{+}$  mice infused with ACSF or FLRF $\alpha$  in conditions of no target and CD1 target ( $n = 9$ –11). ANOVA followed by LSD *post hoc* test: \* $P < 0.05$ , \*\* $P < 0.01$ , \*\*\* $P < 0.001$ . NS, not significant. Data are expressed as the means  $\pm$  s.e.m.

robust  $[Ca^{2+}]_i$  response in cultured Mrg1 $^{+}$  astrocytes and increased ATP concentration in the culture medium by 2.5-fold. We did not observe such an effect in either wild-type astrocytes or Mrg1 $^{+}$  neurons (Supplementary Fig. 15). An FLRF $\alpha$  infusion had no effect in tTA $^{+}$  mice; however, FLRF $\alpha$  infusion dramatically decreased the duration of immobility in Mrg1 $^{+}$  mice when compared with controls (Fig. 3c and Supplementary Figs. 2f and 16). Further experiments were conducted using the CSDS paradigm (Supplementary Fig. 2b). ACSF-treated Mrg1 $^{+}$  mice spent 50% less time in the interaction zone when a caged aggressor was introduced relative to the control group. In contrast, the application of FLRF $\alpha$  completely reversed the expression of these depressive behaviors (Fig. 3d). Together, these results indicate that increased astrocytic ATP release is sufficient to induce antidepressant-like effects in mouse models of depression.

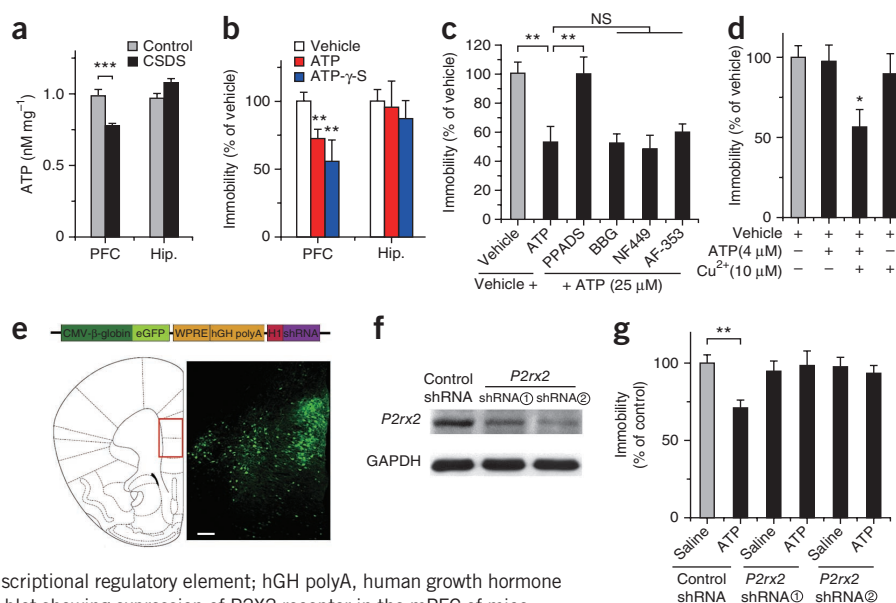
To determine the brain region that mediates the behavioral response to ATP, we first probed a causal link between ATP deficiency and the existing stress-induced, depressive-like states. We found that 7-d CSDS could induce social avoidance behaviors, whereas 1-d CSDS did not (Supplementary Fig. 17). Notably, the ATP level specifically decreased in the PFC from mice subjected to 1-d CSDS (Fig. 4a),

suggesting that the ATP reduction in the PFC was preceded by behavioral changes. Moreover, directly injecting ATP or ATP- $\gamma$ -S into the medial PFC (mPFC), but not into the hippocampus, produced an antidepressant-like effect in the FST (Fig. 4b). Because the regional injection of ATP or ATP- $\gamma$ -S had no effect on locomotor activity (Supplementary Fig. 14b), these results suggest that the mPFC mediates the behavioral response to ATP.

To examine the purinergic receptors involved in the behavioral responses, we first determined the effects of ADP (an agonist of P2Y1, P2Y12 and P2Y13) and UTP (an agonist of P2Y2, P2Y4 and P2Y6) (ref. 25) and found that P2Y receptors were not involved (Supplementary Figs. 14c and 18a). We then blocked P2X receptors with specific receptor antagonists before ATP treatment (Supplementary Fig. 2a). Preinfusion of isopyridoxal-phosphate-6-azophenyl-2',4'-disulfonate (an antagonist of P2X1, P2X2, P2X3, P2X5 and P2X7 receptors)<sup>25,26</sup> into the mPFC blocked the antidepressant-like effect of ATP in the FST, whereas infusion with brilliant blue G (BBG; an antagonist of P2X4, P2X5 and P2X7 receptors)<sup>27</sup>, NF449 (an antagonist of P2X1 receptor)<sup>26</sup> or AF-353 (an antagonist of P2X3 receptor)<sup>28</sup> did not (Fig. 4c). No antagonist alone had an effect on immobility and locomotor

**Figure 4** Prefrontal P2X2 receptors mediate the antidepressant-like effects of ATP.

(a) ATP measurements showing ATP levels in the medium of slices from PFC or hippocampus that were isolated from mice subjected to 1-d CSDS ( $n = 6$  or 7). (b) Quantification of the immobility for the mice injected with ACSF (vehicle), ATP or ATP- $\gamma$ -S into the mPFC or hippocampus ( $n = 8$ ). (c) The effect of the mPFC preinfusion of isopyridoxal-phosphate-6-azophenyl-2',4'-disulfonate (PPADS), BBG, NF449 or AF-353 on the antidepressant-like effect of ATP in the FST ( $n = 9$ ). (d) Quantification of immobility of the mice infused with saline (vehicle), Cu $^{2+}$ , ATP or Cu $^{2+}$  + ATP in the FST ( $n = 10$ ). (e) Schematic of the AAV vector encoding shRNA (top) and the injection site into the mPFC (bottom left, red box, coronal section at +1.78 mm bregma), with an image of eGFP expression in the mPFC 2 weeks after injection (bottom right; scale bar, 100  $\mu$ m). CMV, CMV immediate early promoter;  $\beta$ -globin, human  $\beta$ -globin intron; WPRE, woodchuck hepatitis post-transcriptional regulatory element; hGH polyA, human growth hormone poly-adenylation signal; H1, H1 promoter. (f) Western blot showing expression of P2X2 receptor in the mPFC of mice injected with AAV-shRNAs. (g) Quantification of the immobility of the mice injected with AAV-P2x2 shRNAs or control shRNA followed by an i.p. injection of ATP or saline ( $n = 10$ ). ANOVA followed by LSD *post hoc* test: \* $P < 0.05$ , \*\* $P < 0.01$ , \*\*\* $P < 0.001$ . NS, not significant. Data are expressed as the means  $\pm$  s.e.m.





activity except BBG, which decreased the duration of immobility in the FST (**Supplementary Figs. 14d and 18b**). These results suggest that the P2X2 receptor could be the purinergic receptor subtype that mediates the behavioral response of ATP. Notably, we also found that ATP (4  $\mu$ M) combined with  $\text{Cu}^{2+}$ , a P2X2 receptor enhancer<sup>29</sup>, substantially decreased the total duration of immobility in the FST, whereas ATP (4  $\mu$ M) alone did not (**Fig. 4d and Supplementary Fig. 14e**), providing further support for an involvement of P2X2 receptors in the antidepressant-like effect of ATP. Moreover, adeno-associated virus (AAV)-P2rx2 shRNAs were used to silence endogenous P2X2 receptors in the mPFC (**Fig. 4e,f and Supplementary Fig. 18c,d**). We found that knockdowns of the P2X2 receptor prevented antidepressant-like effects of ATP in the FST (**Fig. 4g and Supplementary Figs. 2g and 14f**). Together, these results demonstrate that activation of P2X2 receptors in the mPFC is required for the antidepressant-like effect of ATP.

That astrocytic ATP release is necessary and sufficient to modulate depressive-like behaviors in adult mice is the major finding of the present study. Histopathological postmortem studies have consistently shown reductions in glial cell density and numbers in the PFC in individuals with MDD<sup>2–4</sup>. Additionally, a microarray-based investigation demonstrated dysregulation of genes involved in ATP biosynthesis and use in the PFC in subjects with MDD<sup>30</sup>. Here, we showed that deficient astrocytic release of ATP induced depressive-like behaviors, whereas stimulating astrocytic ATP release or mPFC infusion of ATP produced antidepressant-like effects in adult mice. Together, these results suggest that astrocytic ATP release has a pivotal role in the biological mechanisms of MDD. Anhedonia is the core symptom of MDD. *Itpr2*<sup>−/−</sup> mice exhibited anhedonia, and treatment with either imipramine or fluoxetine, two well-characterized antidepressants, reversed this depressive behavior, suggesting that *Itpr2*<sup>−/−</sup> mice may be used as a genetic model of depression. In summary, our data suggest that studies that focus on how stress results in decreased astrocytic ATP release will extend the understanding of MDD pathophysiology. Understanding the mechanisms that underlie the antidepressant-like effect of ATP may allow the identification of new targets for the treatment of depression.

## METHODS

Methods and any associated references are available in the [online version of the paper](#).

*Note: Supplementary information is available in the online version of the paper.*

## ACKNOWLEDGMENTS

We thank J. Chen (University of California, San Diego) for providing *Itpr2*<sup>+/−</sup> mice and P.G. Haydon (Tufts University School of Medicine, Boston) for providing GFAP-tTA and tetO.SNARE mouse lines. We thank L. Mei for his insightful suggestions. This work was partly supported by the National Natural Science Foundation of China (grants 81171276, 8103002 and U1201225), the Key Project of Guangdong Province (grants 9351051501000003 and CXZB1018), the Guangzhou Science and Technology Project (grant 7411802013939), the Major State Basic Research Program of China (grant 2012CB518203), the Program for Changjiang Scholars and Innovative Research Team in University (grant IRT1142) and the Project supported by Guangdong Province Universities and Colleges Pearl River Scholar Funded Scheme (2011).

## AUTHOR CONTRIBUTIONS

X.-H.Z. and T.-M.G. designed the research. X.C., L.-P.L., Q. Wang, J.Z., W.-C.X., Y.-B.G., X.-W.L., Y.-Y.F., Y.-N.Z. and H.-C.Y. conducted the behavioral tests and analysis. X.C., L.-P.L., Q. Wu, M.Z. and J.-H.L. performed the ELISA and ATP measurements. X.C. and L.-R.S. contributed to the HPLC analysis. X.C. performed the immunofluorescence, calcium imaging, osmotic minipump implantation and stereotaxic microinjection. L.-P.L., X.C. and S.-J.L. performed the cell culture.

Q. Wu and H.-H.H. performed the western blotting. X.-H.Z., T.-M.G. and X.C. analyzed the data and wrote the paper.

## COMPETING FINANCIAL INTERESTS

The authors declare no competing financial interests.

Reprints and permissions information is available online at <http://www.nature.com/reprints/index.html>.

- Kessler, R.C. *et al.* The epidemiology of major depressive disorder: results from the National Comorbidity Survey Replication (NCS-R). *J. Am. Med. Assoc.* **289**, 3095–3105 (2003).
- Ongür, D., Drevets, W.C. & Price, J.L. Glial reduction in the subgenual prefrontal cortex in mood disorders. *Proc. Natl. Acad. Sci. USA* **95**, 13290–13295 (1998).
- Rajkowska, G. *et al.* Morphometric evidence for neuronal and glial prefrontal cell pathology in major depression. *Biol. Psychiatry* **45**, 1085–1098 (1999).
- Cotter, D., Mackay, D., Landau, S., Kerwin, R. & Everall, I. Reduced glial cell density and neuronal size in the anterior cingulate cortex in major depressive disorder. *Arch. Gen. Psychiatry* **58**, 545–553 (2001).
- Sheline, Y.I., Gado, M.H. & Kraemer, H.C. Untreated depression and hippocampal volume loss. *Am. J. Psychiatry* **160**, 1516–1518 (2003).
- Banasr, M. & Duman, R.S. Glial loss in the prefrontal cortex is sufficient to induce depressive-like behaviors. *Biol. Psychiatry* **64**, 863–870 (2008).
- Banasr, M. *et al.* Glial pathology in an animal model of depression: reversal of stress-induced cellular, metabolic and behavioral deficits by the glutamate-modulating drug riluzole. *Mol. Psychiatry* **15**, 501–511 (2010).
- Berton, O. *et al.* Essential role of BDNF in the mesolimbic dopamine pathway in social defeat stress. *Science* **311**, 864–868 (2006).
- Krishnan, V. *et al.* Molecular adaptations underlying susceptibility and resistance to social defeat in brain reward regions. *Cell* **131**, 391–404 (2007).
- Stockmeier, C.A. *et al.* Cellular changes in the postmortem hippocampus in major depression. *Biol. Psychiatry* **56**, 640–650 (2004).
- Zhang, Q. *et al.* Fusion-related release of glutamate from astrocytes. *J. Biol. Chem.* **279**, 12724–12733 (2004).
- Zou, C.J., Onaka, T.O. & Yagi, K. Effects of suramin on neuroendocrine and behavioral responses to conditioned fear stimuli. *Neuroreport* **9**, 997–999 (1998).
- Monleon, S. *et al.* Attenuation of sucrose consumption in mice by chronic mild stress and its restoration by imipramine. *Psychopharmacology (Berl.)* **117**, 453–457 (1995).
- Surget, A. *et al.* Drug-dependent requirement of hippocampal neurogenesis in a model of depression and of antidepressant reversal. *Biol. Psychiatry* **64**, 293–301 (2008).
- Marpean, L. *et al.* Circadian regulation of ATP release in astrocytes. *J. Neurosci.* **31**, 8342–8350 (2011).
- Sharp, A.H. *et al.* Differential cellular expression of isoforms of inositol 1,4,5-triphosphate receptors in neurons and glia in brain. *J. Comp. Neurol.* **406**, 207–220 (1999).
- Holtzclaw, L.A., Pandhit, S., Bare, D.J., Mignery, G.A. & Russell, J.T. Astrocytes in adult rat brain express type 2 inositol 1,4,5-trisphosphate receptors. *Glia* **39**, 69–84 (2002).
- Hertle, D.N. & Yeckel, M.F. Distribution of inositol 1,4,5-trisphosphate receptor isoforms and ryanodine receptor isoforms during maturation of the rat hippocampus. *Neuroscience* **150**, 625–638 (2007).
- Zhang, Z. *et al.* Regulated ATP release from astrocytes through lysosome exocytosis. *Nat. Cell Biol.* **9**, 945–953 (2007).
- Petravicz, J., Fiocco, T.A. & McCarthy, K.D. Loss of IP3 receptor-dependent  $\text{Ca}^{2+}$  increases in hippocampal astrocytes does not affect baseline CA1 pyramidal neuron synaptic activity. *J. Neurosci.* **28**, 4967–4973 (2008).
- Agulhon, C., Fiocco, T.A. & McCarthy, K.D. Hippocampal short- and long-term plasticity are not modulated by astrocyte  $\text{Ca}^{2+}$  signaling. *Science* **327**, 1250–1254 (2010).
- Pascual, O. *et al.* Astrocytic purinergic signaling coordinates synaptic networks. *Science* **310**, 113–116 (2005).
- Dong, X., Han, S., Zylka, M.J., Simon, M.I. & Anderson, D.J. A diverse family of GPCRs expressed in specific subsets of nociceptive sensory neurons. *Cell* **106**, 619–632 (2001).
- Fiocco, T.A. *et al.* Selective stimulation of astrocyte calcium *in situ* does not affect neuronal excitatory synaptic activity. *Neuron* **54**, 611–626 (2007).
- Jacques-Silva, M.C. *et al.* ATP-gated P2X3 receptors constitute a positive autocrine signal for insulin release in the human pancreatic beta cell. *Proc. Natl. Acad. Sci. USA* **107**, 6465–6470 (2010).
- Khakh, B.S. & North, R.A. Neuromodulation by extracellular ATP and P2X receptors in the CNS. *Neuron* **76**, 51–69 (2012).
- Burnstock, G. Physiology and pathophysiology of purinergic neurotransmission. *Physiol. Rev.* **87**, 659–797 (2007).
- Gever, J.R. *et al.* AF-353, a novel, potent and orally bioavailable P2X3/P2X2/3 receptor antagonist. *Br. J. Pharmacol.* **160**, 1387–1398 (2010).
- Xiong, K. *et al.* Differential modulation by copper and zinc of P2X2 and P2X4 receptor function. *J. Neurophysiol.* **81**, 2088–2094 (1999).
- Klempner, T.A. *et al.* Altered expression of genes involved in ATP biosynthesis and GABAergic neurotransmission in the ventral prefrontal cortex of suicides with and without major depression. *Mol. Psychiatry* **14**, 175–189 (2009).

## ONLINE METHODS

**Mice.** Three to four mice were housed in a plastic cage (300 × 170 × 120 mm) at 24 ± 1 °C. The mice were maintained under standard laboratory conditions (12-h light-dark cycle (lights on from 7:00 a.m. to 7:00 p.m.) with free access to food and water) unless otherwise indicated. All of the experiments were conducted in accordance with the Regulations for the Administration of Affairs Concerning Experimental Animals (China) and were approved by the Southern Medical University Animal Ethics Committee. The behavioral tests were performed by experimenters who were blinded to the experimental group between 1:00 and 4:00 p.m. Male C57BL/6J mice (aged 10–12 weeks) were obtained from the Southern Medical University Animal Center (Guangzhou, China).

IP3R2 knockout (*Itpr2*<sup>-/-</sup>) mice were generated by crossing germline-heterozygous-null mutant *Itpr2*<sup>+/-</sup> mice, which were a kind gift from J. Chen<sup>31</sup>. The offspring were genotyped by PCR using mouse tail DNA and wild-type (5'-GCTGTGCCCAAATCCTAGCACTG-3'; 3'-CATGCAGAGGTCGTGTCACTCAT-5') and mutant allele-specific primers (neospecific primer 5'-AGTGATACAGGGCAAGTTCATAC-3'; 3'-AATGGGTGACCGCTTCCTCGT-5'). The PCR products were visualized with ethidium bromide staining.

The GFAP-tTA and tetO.SNARE mice were generously provided by P.G. Haydon. The generation of dn-SNARE transgenic mice has been described previously<sup>22</sup>. The GFAP-tTA mouse (tTA mouse) contains a glial fibrillary acidic protein (GFAP) promoter that drives expression of the tet-off tetracycline transactivator. The tetO.SNARE line carries a tet operator-regulated dn-SNARE domain (corresponding to amino acids 1–96 of synaptobrevin 2) cassette, as well as LacZ and eGFP reporters. dn-SNARE transgenic mice, in which transgenes for dn-SNARE, LacZ and eGFP are expressed in GFAP-positive astrocytes, were generated by crossing the GFAP-tTA and tetO.SNARE lines. The expression of dn-SNARE, LacZ and eGFP was suppressed in these mice by the application of doxycycline. The mice were mated and reared until 3 weeks of age in the presence of doxycycline (25 µg ml<sup>-1</sup> in drinking water) to prevent any potential developmental effects of transgene expression<sup>32</sup>. The doxycycline administration was either ceased at 3 weeks of age or maintained until 10–12 weeks of age.

The B6.Cg-Tg (tetO-Mrgpra1)1Kdmc/Mmmh (tetO.MrgA1) mouse line was purchased from the Mutant Mouse Regional Resource Center (catalog no. 029882). The hGFAP-tTA:tetO-MrgA1 mice were generated by crossing GFAP-tTA mice with the tetO.MrgA1 mice, which carry a tet operator-regulated MrgA1 receptor allele, as previously described<sup>24</sup>. The MrgA1 receptor is a G<sub>q</sub>-coupled receptor that is expressed in dorsal root ganglion nociceptive sensory terminals in the spinal cord. In these terminals, the receptor is activated by FLRF $\alpha$ , resulting in Ca<sup>2+</sup> release from internal stores<sup>23</sup>. To prevent developmental expression of transgenes, all of these crosses were reared with doxycycline in their drinking water until weaning. hGFAP-tTA:tetO-MrgA1 mice that were maintained without doxycycline are referred to as MrgA1<sup>+</sup> mice.

**Chronic social defeat stress.** For the CSDS protocol, a singly caged mouse (test mouse) was exposed to a different CD1 aggressor mouse (target mouse) for 10 min each day for a total of 10 d. Following 10 min of contact, the test mouse and the aggressor were separated by a plastic divider that contained holes. The divider was placed in the middle of the cage, and the test mouse was exposed to chronic stress in the form of a threat for the next 24 h. The control test (nondefeated) mice were housed in equivalent cages but with members of the same strain. The mice that were placed with the controls were changed daily. The avoidance behaviors were tested using the measures of interaction and avoidance that were used during the defeat protocol. The mice were placed in a novel area with a small animal cage at one end, and their movement was tracked for 2.5 min in the absence of the aggressor. Their movement was then followed for 2.5 min in the presence of the caged aggressor. The duration of time that the mice spent in the interaction zone, as well as other measures, was obtained using EthoVision 7.0 software (Noldus). The apparatus was cleaned with a solution of 70% ethanol in water to remove olfactory cues following each trial, and all of the behavioral tests were conducted in the dark.

To separate the susceptible and unsusceptible subpopulations, the avoidance behaviors were tested 24 h following the final session, and an interaction ratio (time spent in the interaction zone in the presence versus the absence of a target

mouse) of 100 was set as a cutoff. The mice with scores <100 were considered susceptible, and those with scores ≥100 were considered unsusceptible. During the treatment, all of the mice were housed individually following the CSDS protocol, and the avoidance behavior was tested 24 h following the treatment (see **Supplementary Fig. 2** for the details of each experimental schedule). Imipramine (15 mg per kg body weight, i.p.) was used as the positive control.

**ELISA.** Twenty-four hours following the CSDS protocol, the mice were deeply anesthetized. Transverse PFC (400 µm, four slices in total) and hippocampal slices (400 µm, ten slices in total) were cut from each mouse brain and transferred into a tube containing 800 µl of an ice-cold oxygenized ACSF solution (containing, in mM, 125 NaCl, 2.5 KCl, 2 CaCl<sub>2</sub>, 2 MgSO<sub>4</sub>, 1.25 NaH<sub>2</sub>PO<sub>4</sub>, 26 NaHCO<sub>3</sub> and 10 D-glucose), which was collected 12 min later for the ELISAs according to the manufacturers' protocols. Mouse TNF- $\alpha$ , IL-6 and TSP-1 ELISA kits were purchased from Boster, and a mouse bFGF ELISA kit was purchased from RayBiotech Inc. Mouse BDNF, GDNF and TGF- $\beta$ 1 EmaxImmunoAssay systems were obtained from Promega.

**HPLC analysis.** HPLC analyses were performed to determine aspartate, glutamate, serine, glutamine, glycine and GABA levels. The compounds, including all of the standards, were purchased from Sigma-Aldrich, unless otherwise indicated. HPLC-grade water and acetonitrile were obtained from Thermo Fisher Scientific. The HPLC system consisted of a model G1354A quaternary pump (Agilent 1200), an Agilent/1322A micro vacuum degasser, an Agilent/G1316A thermostat, an Agilent/G1329A autosampler, a Hipsil ODS column (5-µm particle size, 4 × 125 mm) and an Agilent/G1321A fluorescence detector. The precolumn derivatization of the sample was performed using an o-phthalaldehyde (OPA)/9-fluorenylmethyloxycarbonyl chloride (FMOC) reagent. Briefly, 2 µl of borate buffer (0.1 M, pH 10.5) and 2 µl OPA (0.08 M) were added to and mixed with the 1-µl samples using the microsampler. The reagent was added to and mixed with 1 µl of FMOC (0.01 M) after 60 s. Following another 60-s reaction period in the microsampler, 1 µl of the mixture was injected onto the column. The mobile phase A consisted of 10 mM phosphate-buffered saline (PBS) containing 0.5% (v/v) tetrahydrofuran (pH 7.2), and the mobile phase B consisted of a PBS-methanol-acetonitrile solution (50:35:15, v/v). The following elution program was used following a 1-µl sample injection: 100% A with 0% B at the beginning of the program (0 min) and 0% A with 100% B at the end (25 min) of the program, with a flow rate of 1 ml min<sup>-1</sup>. The column was maintained at a temperature of 40 °C. The detection limit was 1 pmol per injection. The quantification was performed using peak area ratios from calibration standard curves and was normalized to the total protein levels in the brain slices as determined using a BCA protein assay kit (Thermo Fisher Scientific).

**Extracellular ATP measurement.** The ATP levels were determined using a bioluminescent ATP assay kit (Promega), as previously described<sup>33</sup>. The ectonucleotidase inhibitor 6-N,N-diethyl- $\beta$ - $\gamma$ -dibromomethylene-D-adenosine-5-triphosphate FPL 67156 (ARL 67156 trisodium salt) was added to the extracellular solution or the conditioned medium throughout the experiment to decrease ATP hydrolysis. Luminescence was measured using a luminometer (PerkinElmer) according to the manufacturer's instructions. A calibration curve was obtained from standard ATP samples, and the luminescence of normal culture medium was considered to be the background ATP level. For ATP release measurements in acute hippocampal and PFC slices, the slices were incubated in ice-cold oxygenized ACSF for 12 min. The ACSF was then collected for the ATP assay. For quantification, protein amounts were normalized to the total protein of each sample.

**Microdialysis.** Twenty-four hours following the CSDS protocol, each mouse was then deeply anesthetized and mounted on the stereotaxic frame (Stoelting). A guide cannula (CMA/7, CMA/Microdialysis) was implanted into the right mPFC (15° angle, anteroposterior (AP) = +1.75 mm; mediolateral (ML) = 0.75 mm; dorsoventral (DV) = 1.5 mm) or the hippocampus (AP = -2.0 mm; ML = 1.2 mm; DV = 1.2 mm). A microdialysis probe (CMA/7, membrane length: 1–2 mm, molecular weight cut-off: 6,000 Da, outer diameter: 0.24 mm) was inserted through the guide cannula and connected to the syringe pump

(CMA 402). The ASCF was continuously perfused through the microdialysis probe at a constant flow rate of  $1 \mu\text{l min}^{-1}$ , and sampling was performed 1 h following the insertion of probe. Two samples ( $60 \mu\text{l}$  each) were automatically collected from each mouse using the CMA 142 microfraction collector every 60 min over 120 min. To decrease the rate of background ATP hydrolysis, each sample collection tube was pretreated with ARL 67156 ( $1 \mu\text{l}$ ), and the interstitial fluid ATP levels were measured immediately.

**Stereotaxic microinjection.** The mice were anesthetized and placed in a stereotaxic frame. A brain infusion cannula (PlasticsOne) was unilaterally implanted in the right cerebral ventricle (AP =  $-0.6$ , ML =  $1.5$  mm, DV =  $2.0$  mm,  $5 \mu\text{l}$ ,  $0.5 \mu\text{l min}^{-1}$ ), mPFC (AP =  $+1.75$ , ML =  $0.75$ , DV =  $2.65$ ,  $1 \mu\text{l}$ ,  $0.1 \mu\text{l min}^{-1}$ ) or hippocampus (AP =  $-2.0$  mm, ML =  $1.2$  mm, DV =  $2$  mm,  $1 \mu\text{l}$ ,  $0.1 \mu\text{l min}^{-1}$ ). Seven days after implantation, vehicle, ATP ( $25 \mu\text{M}$ ), ATP- $\gamma$ -S ( $50 \mu\text{M}$ ), suramin ( $1.5$  mM), FLRF $\alpha$  ( $10 \mu\text{M}$ ), ADP ( $10$ ,  $25$ ,  $50$  and  $125 \mu\text{M}$ ), UTP ( $10$ ,  $25$ ,  $50$  and  $125 \mu\text{M}$ ), isopyridoxal-phosphate-6-azophenyl-2', 4'-disulfonate (PPADS) ( $50 \mu\text{M}$ ), BBG ( $10 \mu\text{M}$ ), NF449 ( $1 \mu\text{M}$ ), AF-353 ( $0.1 \mu\text{M}$ , dissolved in  $0.1\%$  DMSO) or  $\text{Cu}^{2+}$  ( $10 \mu\text{M}$ , as  $\text{CuCl}_2$  dissolved in saline) combined with ATP ( $4 \mu\text{M}$ ) was delivered using an automatic injector (catalog no. 53311, Stoelting) into the lateral ventricles, mPFC or hippocampus of free-moving mice. The behavioral test was conducted 30 min following the infusion. All compounds were dissolved in ACSF unless otherwise indicated.

**Osmotic minipump implantation.** The mice were subjected to the 10-d CSDS protocol. Following 3 d of recovery, each mouse was anesthetized and an osmotic pump (Model 1007D, Alzet) was implanted in the right lateral cerebral ventricle. The osmotic pumps are designed to deliver a flow rate of  $0.5 \mu\text{l h}^{-1}$  for 7 d and were filled with ACSF, ATP ( $2.5$  mM), ATP- $\gamma$ -S ( $5$  mM), or FLRF $\alpha$  ( $0.5$  mM), the latter three of which were dissolved in ACSF. Social avoidance behaviors were tested 7 d following the implantation (Supplementary Fig. 2b).

**Forced swimming test.** The FST was performed in a clear glass cylinder (height  $45$  cm, diameter  $19$  cm), which was filled to  $23$  cm with water ( $22$ – $25^\circ\text{C}$ ). The test lasted for 6 min. The duration of immobility was recorded during the final 4 min by an investigator who was blinded to the study conditions. In the drug treatment conditions, imipramine ( $15$  mg per kg body weight, i.p.) and fluoxetine ( $20$  mg per kg body weight, i.p.) were used as the positive controls; the FST was conducted 30 min following the injection.

**Open field test.** The open field apparatus consisted of a rectangular chamber ( $40 \times 40 \times 30$  cm) that was made of gray polyvinyl chloride. A video camera, a loudspeaker that provided masking noise and a  $25$  W red light bulb (illumination density at the center of the maze,  $0.3$  lx) were placed  $180$  cm above the center of the apparatus. The mice were gently placed on the center and left to explore the area for 5 min. The digitized image of the path taken by each mouse was stored, and the locomotion activity and number of rearings were analyzed *post hoc* using EthoVision 7.0 software.

**Elevated-plus-maze test.** The elevated-plus-maze test consisted of two opposing open arms ( $30 \times 5 \times 0.5$  cm) and two opposing enclosed arms ( $30 \times 5 \times 15$  cm) that were connected by a central platform ( $5 \times 5$  cm), forming the shape of a plus sign. All of the measurements were taken in a dimly lit experimental room, in which the mice were acclimatized for at least 30 min before testing. The times that were spent in the open arms and the enclosed arms were recorded over a 5-min test period. The maze was cleaned with a solution of 20% ethanol in water between the sessions.

**Coat score assay.** Accumulating evidence indicates that the coat state is a reliable and well-validated metric in mouse models of depression<sup>14,34</sup>. The physical state of the fur was evaluated daily or weekly, and the total coat score was measured as the sum of the score of seven different body parts: head, neck, dorsal coat, ventral coat, tail, forepaws and hindpaws. For each of the seven areas, a score of 1 was given for a well-groomed coat and a score of 0 was given for an unkempt coat.

**Sucrose preference.** Two sucrose preference test procedures were used in this study. To examine the depressive behaviors of *Itpr2*<sup>-/-</sup> mice (10–12 weeks of age), an 8-d sucrose preference protocol was used<sup>35</sup>. Briefly, the mice were singly caged 3 d before the test, after which their normal water bottles were replaced with two 50-ml bottles (A and B). The bottle positions were switched daily to avoid a side bias. The mice were habituated for 4 d to a 1% sucrose solution as follows: during days 1 and 2, bottles A and B were filled with water (w/w), and on days 3 and 4, bottles A and B were filled with 1% sucrose solution (s/s). The sucrose preference test was conducted between days 5 and 8. On the test days, bottle A contained 1% sucrose solution, and bottle B contained water (s/w). The fluid that was consumed from each bottle was measured daily. The sucrose preference on each day for each mouse was calculated as  $100 \times (\text{Vol}_A / (\text{Vol}_A + \text{Vol}_B))$ , and the total fluid intake was calculated as  $\text{Vol}_A + \text{Vol}_B$ .

For the drug treatment experiments, the mice were habituated for 2 d to 1% sucrose as follows: on day 1, bottles A and B were filled with water (w/w), and on day 2, bottles A and B were filled with 1% sucrose solution (s/s). Starting one day following the habituation protocol, the sucrose preference was determined weekly for 1 h following a 22-h period of water and food deprivation. Three tests were performed to stabilize the sucrose preference baseline, and treatments began at the end of the third test.

**Chronic mild stress.** Mice were singly caged and habituated to 1% sucrose solution for 2 d as described above. The physical state of each mouse's fur and its sucrose preference were tested weekly, and the measurements of the three tests were used as the baseline. Following the third test, the mice were matched according to their sucrose preference scores and coat scores and divided into three groups: control, saline treated and ATP treated. The mice were then subjected to a CMS protocol<sup>14,36</sup> (Supplementary Fig. 3d). Briefly, this protocol consisted of the sequential application of a variety of mild stressors, including restraint (4 h), forced swim in ice-cold water (5 min), food and water deprivation (24 h), cage tilting ( $45^\circ$ , three times, 12 h each), reversal of the light-dark cycle (one time), strobe light (12 h) and soiled cage (two times, 14 h each). This schedule lasted for 6 weeks. For the treatment protocol, ATP ( $125$  mg per kg body weight, i.p.) or saline (i.p.) was administered for 3 weeks. The mice that were housed in the adjacent room were used as controls.

**Virus generation and stereotaxic injections.** AAV was produced by transfection of 293T cells with three plasmids: an AAV vector expressing the shRNA to *P2rx2* and EGFP or EGFP alone, AAV helper plasmid (pAAV Helper) and AAV Rep/Cap expression plasmid. At 72 h after transfection, the cells were collected and lysed using a freeze-thaw procedure. Viral particles were purified by an iodixanol step-gradient ultracentrifugation method. The iodixanol was diluted, and the AAV was concentrated using a  $100$ -kDa molecular-mass-cutoff ultrafiltration device. The genomic titer was  $2.5 \times 10^{12}$ – $3.5 \times 10^{12}$  infectious unit per ml determined by quantitative PCR. To construct shRNAs, oligonucleotides that contained 21-base sense and antisense sequences were connected with a hairpin loop followed by a poly (T) termination signal. The sequences targeting *P2rx2* (GenBank accession: [NM\\_153400](#)) that were used in the experiments were 5'-GCAGGGAAATTCAGTCTCATT-3' and 5'-CCAAAGGTTTGGCCCAACTTT-3'. The sequence of the control shRNA was TTCTCCGAACGTGTACAGT. These shRNAs were ligated into an AAV8 vector expressing EGFP. For *in vivo* viral injections, viral vectors were bilaterally targeted to the mPFC. Specifically, a Hamilton syringe fitted with a 33-gauge needle was filled with  $1.5 \mu\text{l}$  of virus. The needle was lowered into the mPFC, and  $0.4 \mu\text{l}$  of virus was delivered over 4 min. After a 5-min delay, the needle was pulled up  $0.25$  mm and an additional  $0.4 \mu\text{l}$  of virus was delivered over an additional 4 min. The injection needle was withdrawn 5 min after the second infusion. Mice were used 2 weeks after AAV injections.

**Statistical analyses.** All of the results are expressed as the means  $\pm$  s.e.m. The statistical analyses were performed using SPSS 13.0 software. Potential differences between the mean values were evaluated using one-way analysis of variance (ANOVA) followed by the least significant difference (LSD) test for *post hoc* comparisons when equal variances were assumed. Independent-sample *t*-tests were used to compare differences between any given two groups.



throughout the study, unless otherwise specified. The significance level for all of the tests was set at  $P < 0.05$ .

31. Li, X., Zima, A.V., Sheikh, F., Blatter, L.A. & Chen, J. Endothelin-1-induced arrhythmogenic  $\text{Ca}^{2+}$  signaling is abolished in atrial myocytes of inositol 1,4,5-trisphosphate (IP3) receptor type 2-deficient mice. *Circ. Res.* **96**, 1274–1281 (2005).
32. Halassa, M.M. *et al.* Astrocytic modulation of sleep homeostasis and cognitive consequences of sleep loss. *Neuron* **61**, 213–219 (2009).
33. Cotrina, M.L. *et al.* Connexins regulate calcium signaling by controlling ATP release. *Proc. Natl. Acad. Sci. USA* **95**, 15735–15740 (1998).
34. Alonso, R. *et al.* Blockade of CRF (1) or V(1b) receptors reverses stress-induced suppression of neurogenesis in a mouse model of depression. *Mol. Psychiatry* **9**, 278–286, 224 (2004).
35. Roybal, K. *et al.* Mania-like behavior induced by disruption of CLOCK. *Proc. Natl. Acad. Sci. USA* **104**, 6406–6411 (2007).
36. Monleon, S. *et al.* Attenuation of sucrose consumption in mice by chronic mild stress and its restoration by imipramine. *Psychopharmacology (Berl.)* **117**, 453–457 (1995).